Soft Matter

PAPER

View Article Online
View Journal | View Issue

Check for updates

Cite this: *Soft Matter*, 2024, **20**, 2126

Mechanochromic polymer blends made with an excimer-forming telechelic sensor molecule†

Marta Oggioni, [a] Jess M. Clough [ab] and Christoph Weder *[ab]

Received 5th November 2023,
Accepted 5th February 2024

DOI: 10.1039/d3sm01489d

rsc.li/soft-matter-journal

The ability to monitor mechanical stresses and strains in polymers *via* an optical signal enables the investigation of deformation processes in such materials and is technologically useful for sensing damage and failure in critical components. We show here that this can be achieved by simply blending polymers of interest with a small amount of a mechanochromic luminescent additive (**Py-PEB**) that can be accessed in one step by end-functionalizing a telechelic poly(ethylene-*co*-butylene) (PEB) with excimer-forming pyrenes. **Py-PEB** is poorly miscible with polar polymers, such as poly(ε-caprolactone) and poly(urethane), so that blends undergo microphase separation even at low additive concentrations (0.1–1 wt%), and the emission is excimer-dominated. Upon deformation, the ratio of excimer-to-monomer emission intensity decreases in response to the applied stress or strain. The approach appears to be generalizable, although experiments with poly(isoprene) show that it is not universal and that the (in)solubility of the additive in the polymer must be carefully tuned.

Open Access Article. Published on 06 February 2024. Downloaded on 9/15/2025 9:44:22 AM.
This article is licensed under a Creative Commons Attribution-NonCommercial 3.0 Unported Licence.

Introduction

The ability to monitor mechanical stresses and strains in polymeric materials *via* an easily detectable optical signal enables the investigation of deformation processes and is technologically useful, for example, in pressure-sensing films, tamper-evident packaging solutions, and damage sensing.[1–3] The most widely employed approach to impart polymers with mechanochromic characteristics is the covalent incorporation of so-called mechanophores,[4] *i.e.*, molecular motifs that undergo mechanically triggered chemical reactions,[5–9] conformational changes,[10,11] rearrangements of interacting optically active moieties,[12–15] or other effects that cause reversible or irreversible changes to the motif's optical absorption and/or photoluminescence.[14,16–19] This general approach has the fundamental disadvantage that chemical modifications are required to render a polymer of interest mechanochromic. Such modifications are often not possible by post-polymerization processes, and therefore the preparation of mechanochromic polymers generally requires *de novo* synthesis. A much simpler approach involves the blending of polymers with optically active compounds, whose optical properties change when the material is subjected to mechanical forces.[20] This concept was first introduced two decades ago by Löwe and Weder, who incorporated excimer-forming, photoluminescent oligo(*p*-phenylene vinylene) dyes (cyano-OPVs) into polyethylene.[21,22] The deformation of these blends causes the dissociation of aggregated dye molecules, which in turn leads to a pronounced change of the photoluminescence colour. Such emission changes represent an attractive readout, as they are often not only visually detectable, but can easily be measured and the recorded spectrum (unlike a change in the fluorescence intensity) is independent of sample dimensions and the acquisition geometry.[21–25] This framework was subsequently applied to different excimer-forming[26] and aggregachromic dyes[27] and exploited in several matrix polymers.[28] However, a significant limitation of using nanoscale aggregates of small-molecule dyes is that it requires that the mechanochromic additive forms nanoscale aggregates in the polymer matrix and that such aggregates can be mechanically dispersed.[2,20] In many polymers, these conditions are difficult or impossible to satisfy. While the approach generally works well in semi-crystalline polymers, where nucleation effects can promote the formation of small dye aggregates, it is difficult to realize in amorphous materials, where the aggregate formation is hard to control and, if the glass transition temperature is low, the mechanical forces that the aggregates experience may be too small to cause their breakup.[29,30] To address these problems, some of us recently devised a mechanochromic additive that was accessed by end-functionalizing a telechelic poly(ethylene-*co*-butylene) (PEB) with excimer-forming cyano-OPVs.[31] This design was originally based on the hypothesis that the additive's PEB blocks might entangle with the chains of the matrix polymer. Such entanglements were thought to limit the size of the OPV aggregates and facilitate efficient stress transfer between the matrix and the mechanochromic additive. Blends of different polymers, including poly(ε-caprolactone), poly(isoprene), poly(styrene-*b*-butadiene-*b*-styrene), and different thermoplastic

[a] *Adolphe Merkle Institute, University of Fribourg, Chemin des Verdiers 4, Fribourg CH-1700, Switzerland. E-mail: christoph.weder@unifr.ch*
[b] *National Center of Competence in Research Bio-inspired Materials, Chemin des Verdiers 4, Fribourg CH-1700, Switzerland*

† Electronic supplementary information (ESI) available. See DOI: https://doi.org/10.1039/d3sm01489d

This journal is © The Royal Society of Chemistry 2024

Open Access Article. Published on 06 February 2024. Downloaded on 9/15/2025 9:44:22 AM.
This article is licensed under a Creative Commons Attribution-NonCommercial 3.0 Unported Licence.

polyurethanes, and 0.1–2% w/w of the telechelic additive indeed all display mechanochromic luminescence.[31,32] However, the mechanism that causes this effect was shown to be different than originally hypothesized. On the basis of confocal laser scanning microscopy experiments, it was demonstrated that mixtures of the various matrices and the telechelic additive undergo microphase separation to form discrete spherical inclusions.[33] These droplets have radii in the range of 400–900 nm and consist of mixtures of the host polymer and the additive. In the unstretched state, the photoluminescence of these droplets is dominated by excimer emission. However, upon deformation of the blends, the inclusions deform,[34] and this reduces the extent of excimer emission. The deformation of the inclusions follows Eshelby's inclusion theory,[34] which allows the mechanical properties of the droplets to be determined by relating the change in their shape to the macroscopically applied strain. The inclusions were softer than the surrounding matrices, elongate upon deformation, and this shape change causes a decrease in excimer emission. With the goals of demonstrating that the approach is generalizable and simplifying the synthesis of the sensor molecule, we set out to prepare a pyrene-terminated PEB telechelic and investigated the mechanochromic response of polymers containing this additive.

Results and discussion

From the plethora of luminophores that might be useful to create the targeted telechelic mechanochromic sensor molecules, we selected pyrene, one of the most widely investigated excimer-forming emitters.[35] Pyrene has previously been used to render different polymers mechanochromic, for example by covalently attaching the dye to poly(dimethylsiloxane),[36,37] to styrene-*b*-(ethylene-*co*-butylene)-*b*-styrene triblock copolymer,[38] or to water-soluble PEG-based cross-linkers for hydrogels.[39] While elegant and effective, the aforementioned approaches comprise additional synthetic steps to endow the selected polymers with mechanochromism. Our choice was in part motivated by the fact that several functionalized pyrene derivatives are commercially available, and this allowed us to access a pyrene-terminated PEB (**Py-PEB**, Fig. 1 and ESI,† Fig. S1) in one synthetic step. Thus, we esterified dihydroxy-terminated PEB with a number-average molecular weight (M_n) of 3100 kg mol^{-1} with 1-pyrenebutyric acid. This was achieved by adapting a literature protocol and using dicyclohexylcarbodiimide and 4-dimethylaminopyridine as coupling agents (see ESI† for details).[40] Nuclear magnetic resonance (NMR) spectra reveal that for the isolated fraction (32% yield, no attempts to improve the yield were made), the esterification is quantitative, while size-exclusion chromatography traces acquired with different detectors confirm the covalent attachment of the pyrene moieties to the PEB backbone (Fig. S2 and S3, ESI†). The successful esterification is also confirmed by the appearance of a sharp carbonyl band at 1738 cm^{-1} in FTIR spectra (Fig. S4, ESI†).

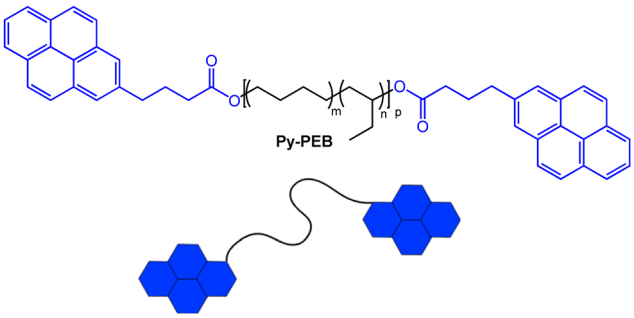

Fig. 1 Chemical structure of the pyrene-terminated poly(ethylene-*co*-butylene) telechelic **Py-PEB** ($m \approx 0.36$, $n \approx 0.64$, $p \approx 55$).

The photoluminescence spectrum of a solution of **Py-PEB** (c = 1 μmol L^{-1}) shows the characteristic monomer emission of pyrene, with well-resolved phonon bands at 376, 397, and 420 nm. The spectrum is almost identical to that of a 2 μmol L^{-1} solution of 1-pyrenebutanol, which we used as a reference compound that does not show any excimer emission at this concentration. By contrast, the emission spectrum of the bulk **Py-PEB** material, which at ambient temperature is a viscous liquid, displays primarily a broad emission band around 475 nm that is diagnostic of pyrene excimers (Fig. S5b, ESI†).[35] Since intramolecular encounters of the end groups of such telechelics dominate over intermolecular interactions only in highly dilute solutions,[41] the excimer emission in the **Py-PEB**/polymer blends must be caused by intermolecular assembly, and is possibly facilitated by microphase separation of the pyrenyl groups. Moreover, the differential scanning calorimetry (DSC) trace of **Py-PEB** shows only a glass transition at −44 °C, slightly higher than the parent OH-PEB (−50 °C), and is void of any other thermal transitions (Fig. S6b, ESI†). Thermogravimetric analysis (TGA) traces show that **Py-PEB** displays high thermal stability, with a degradation onset temperature of 326 °C (Fig. S7, ESI†).

Blends of three commercially available polymers and **Py-PEB** were prepared by solvent-casting THF solutions and solvent evaporation. Semicrystalline *trans*-poly(isoprene) (PI), which was blended with 0.5–10 wt% **Py-PEB**, poly(ε-caprolactone) (PCL) that was formulated with 0.5 or 1 wt% **Py-PEB**, and a poly(urethane) (PU) elastomer that was mixed with 0.1–1 wt% **Py-PEB** were chosen to (i) probe the effectiveness of **Py-PEB** in nonpolar (PI) and polar (PCL, PU) matrices, (ii) explore the capability of monitoring irreversible deformation of a semicrystalline plastic (PI, PCL) and reversible deformation of an elastomer (PU), and (iii) enable the comparison with previous studies that involved the same matrix polymers, but a cyano-OPV terminated telechelic.[31,32] PI/**Py-PEB*x*** and PCL/**Py-PEB*x*** blends were processed into *ca.* 100 μm thin films by compression-moulding at 100 °C (subscript ***x*** denotes the **Py-PEB** content in wt%) whereas PU/**Py-PEB*x*** films were prepared *via* solvent casting.

Fig. 2a displays normalized photoluminescence spectra of films made with PI/**Py-PEB** blends with a **Py-PEB** content of 0.5–10 wt%. The data shows that the excimer emission

Open Access Article. Published on 06 February 2024. Downloaded on 9/15/2025 9:44:22 AM.
This article is licensed under a Creative Commons Attribution-NonCommercial 3.0 Unported Licence.

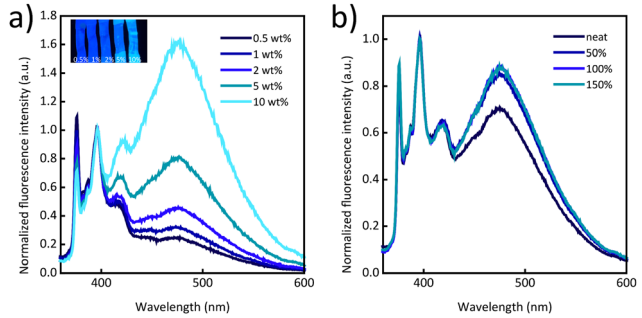

Fig. 2 (a) Photoluminescence spectra of PI/**Py-PEB** blend films with a **Py-PEB** content of 0.5–10 wt%. The inset shows a picture of stretched films taken under illumination with 365 nm UV light. (b) Photoluminescence spectra of a PI/**Py-PEB**$_5$ film that was uniaxially deformed to the indicated strain. All spectra were acquired upon excitation at 310 nm and were normalized to the intensity of the monomer peak at 397 nm.

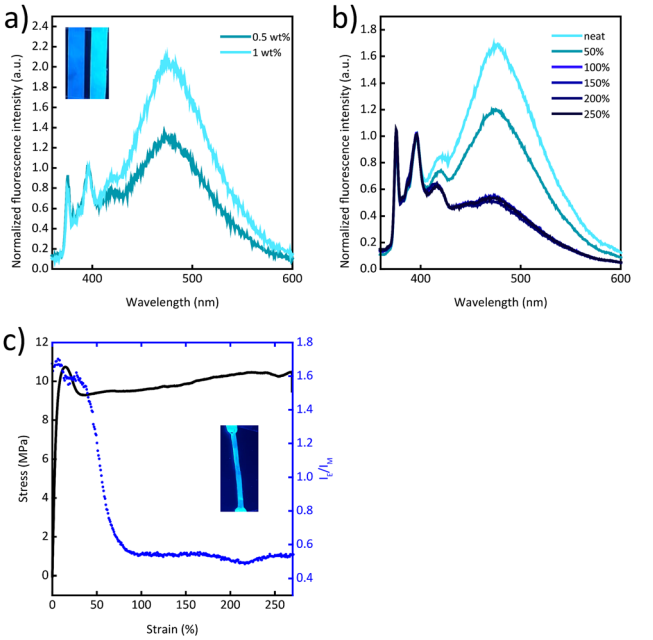

Fig. 3 (a) Photoluminescence spectra and photograph of PCL/**Py-PEB** blend films with a **Py-PEB** content of 0.5 or 1 wt%. (b) Photoluminescence spectra of a PCL/**Py-PEB**$_1$ film that was uniaxially deformed to the indicated strain. (c) Stress–strain curve and excimer-to-monomer emission intensity ratio (I_E/I_M) recorded at 475 and 397 nm of a PCL/**Py-PEB**$_1$ film. The inset shows a picture of a deformed film under excitation at 365 nm. All spectra were acquired upon excitation at 310 nm and were normalized to the intensity of the monomer peak at 397 nm.

increases with the content of the telechelic and becomes dominant at a **Py-PEB** content of 10 wt%. Stretching PI/**Py-PEB**$_5$ films up to 150% strain does not cause a reduction of the excimer emission (Fig. 2b and Fig. S8a, b, ESI†), which contrasts with the results of a previous investigation of PI blends containing an otherwise similar cyano-OPV terminated PEB telechelic. Even at a low additive concentration of 0.5 wt% the previously studied blends display mostly excimer emission,[31] as the additive phase separated from the matrix, forming spherical inclusions with sub-micrometre radii. As a result of the deformation of these inclusions, the ratio of excimer-to-monomer intensity (I_E/I_M) was considerably reduced upon deformation.[33] The emission spectra of PI/**Py-PEB** blend films shown in Fig. 2a suggest that the solubility of **Py-PEB** in the nonpolar PI matrix is much higher than that of the corresponding cyano-OPV terminated PEB telechelic. Thus, the nature of the luminescent end groups can significantly impact the miscibility of the two components and therefore the blends' morphology, at least in case of nonpolar matrices. Accordingly, we were unable to observe the formation of any inclusions, or any other phase-separated morphology, in PI/**Py-PEB** blend by widefield fluorescence microscopy, even at a **Py-PEB** content of 10 wt% (Fig. S11a and b, ESI†).

Gratifyingly, blends of **Py-PEB** and the more polar PCL mirror the behaviour of previously reported blends of PCL and the cyano-OPV terminated PEB telechelic more closely. In this case, the photoluminescence spectra are dominated by excimer emission at a **Py-PEB** content of as low as 0.5 wt% (Fig. 3a) and fluorescence microscopy images suggest the formation of spherical particles (Fig. S11e, ESI†). Photoluminescence spectra recorded after irreversibly deforming PCL/**Py-PEB**$_1$ films by stretching them past the yield point reveal a clear change from excimer-dominated to monomer-dominated emission (Fig. 3b and Fig. S9, ESI†). To probe this behaviour further, we subjected PCL/**Py-PEB**$_1$ films to tensile tests and simultaneously monitored I_E/I_M at 475 and 397 nm by *in situ* photoluminescence spectroscopy (Fig. 3c). The stress–strain curves reveal that the films deform elastically before they neck at a strain of *ca.* 15% and then plastically deform with little strain hardening. The I_E/I_M *vs.* strain trace appears to capture this behaviour well; I_E/I_M drops from 1.7 to 1.6 in the elastic regime, and from 1.6 to 0.53 upon plastic deformation. The fact that I_E/I_M continues to decrease beyond the yield point up to *ca.* 90% strain is likely related to experimental limitations, *i.e.*, the photoluminescence measurement, which probes a small area of the sample (*ca.* 10 mm^2), may initially average over necked and non-necked regions of the sample, which show different emission characteristics (Fig. S12 and S13, ESI†). A photograph of a stretched PCL/**Py-PEB**$_1$ film shows the corresponding change in photoluminescence colour (Fig. 3c, inset).

Mechanochromic behaviour was also observed for the PU/**Py-PEB** blend films. In this matrix, the solubility of **Py-PEB** appears to be further reduced, as reflected by the fact that blends containing only 0.1 to 0.2 wt% of **Py-PEB** display a significant extent of excimer emission (Fig. 4a). Moreover, fluorescence microscopy images reveal unequivocally the occurrence of microphase separation and the formation of spherical particles that have diameters of the order of 1 μm (Fig. S11c and d, ESI†). The uniaxial deformation of PU/**Py-PEB**$_{0.2}$ films is accompanied by a decrease in the excimer emission (Fig. 4b, c and Fig. S10a, b, ESI†), but in this case, the response is reversible. A cycling deformation experiment was performed, which shows that I_E/I_M decreases after stretching, and quickly recovers upon relaxation, over at least 4 stretch-and-release cycles (Fig. S14a, ESI†).

Finally, a stress relaxation experiment was performed, in which a PU/**Py-PEB**$_{0.2}$ film was stretched to a strain of *ca.* 200% and kept under fixed strain for 3 h (Fig. 4d). Upon deforming the film at a

This journal is © The Royal Society of Chemistry 2024

Open Access Article. Published on 06 February 2024. Downloaded on 9/15/2025 9:44:22 AM.
This article is licensed under a Creative Commons Attribution-NonCommercial 3.0 Unported Licence.

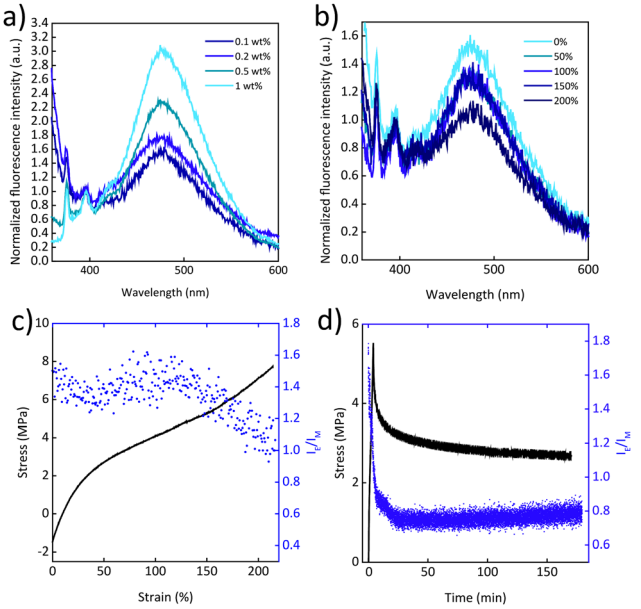

Fig. 4 (a) Photoluminescence spectra of PU/**Py-PEB** blend films with a **Py-PEB** content of 0.1–1 wt%. (b) Photoluminescence spectra of a PU/**Py-PEB**$_{0.2}$ film that was uniaxially deformed to the indicated strain. (c) Stress–strain curve and excimer-to-monomer emission intensity ratio (I_E/I_M) recorded at 475 and 397 nm of a PU/**Py-PEB**$_{0.2}$ film. All spectra were acquired upon excitation at 310 nm and were normalized to the intensity of the monomer peak at 397 nm. (d) Stress relaxation experiment of a PU/**Py-PEB**$_{0.2}$ film. The film was stretched to a strain of *ca.* 200% at a strain rate of 50% min^{-1} and the strain was then fixed and the stress and I_E/I_M were monitored over the course of 3 h.

strain rate of 50% min^{-1}, the I_E/I_M value decreases, as already shown in Fig. 4c. When kept at a constant strain, stress relaxation occurs and I_E/I_M increases slightly. While the stress decays nonlinearly with time, the increase of I_E/I_M shows a linear time dependence.

Conclusions

In summary, we demonstrated that the previously reported[31] excimer-forming, telechelic sensor molecule approach is, in principle, generalizable to other excimer-forming dyes. We report the facile, one-step synthesis of **Py-PEB**, a pyrene-capped, excimer-forming telechelic additive that is useful to render *some* polymeric matrices mechanochromic. However, while small quantities (0.2–1 wt%) of **Py-PEB** imparted the more polar PCL and PU matrices with mechanochromic behaviour, the new additive is highly miscible with the non-polar PI, and this impeded the formation of excimer-forming inclusions. The results thus suggest that the specific design of the telechelic additive is important, in particular with respect to the (in)solubility profile that the dye molecules and the telechelic core impart.

Experimental section

Materials and instrumentation

All reagents and solvents were used without further purification. 1-Pyrenebutyric acid, 1-pyrenebutanol, *N*,*N*′-dicyclohexylcarbodiimide (DCC), 4-dimethylaminopyridine (DMAP), Sudan Black B, poly(caprolactone) (average M_n 80 000 kg mol^{-1}), *trans*-1,4-poly(isoprene) were purchased from Sigma-Aldrich. Dry dichloromethane (DCM) (99.8%, extra dry) was purchased from Acros Organics. Tetrahydrofuran (THF) and toluene were purchased from Fisher Scientific. Polyurethane (PU) (Texin 985®, average M_n = 111 000 kg mol^{-1}) was obtained from Covestro. Bio-Beads™ SX-1 (200–400 mesh) were purchased from Bio-Rad. Dihydroxyl-terminated poly(ethylene-*co*-butylene) (OH-PEB) (average M_n = 3100 kg mol^{-1}), commercial name Krasol HLBH-P 3000, was received from Cray Valley Company.

Nuclear magnetic resonance (NMR) spectroscopy was carried out on a Bruker Avance DPX 400 spectrometer at a frequency of 400.19 MHz for ^{1}H-NMR measurements and of 100.63 MHz for ^{13}C-NMR measurements. The solvent peak of $CDCl_3$ was used to calibrate the spectra. Data were evaluated with the MestReNova software suite (v 12.0).

Size-exclusion chromatography (SEC) measurements were performed on an Agilent 1200 series HPLC system. The column system was composed of a PLgel mixed guard column (particle size 5 μm) and two Agilent PLgel mixed-D columns (ID = 7.5 mm, L = 300 mm, particle size = 5 μm). The detectors used were a UV detector (Agilent 1200 series) and an Optilab REX interferometric refractometer. Samples for SEC were prepared in THF with a concentration of *ca.* 1.5 mg mL^{-1}.

UV-Vis absorption spectra were acquired on a JASCO V670 spectrometer. Data were evaluated on the Spectra Manager software. Quartz cuvettes (1 cm diameter) were used to measure absorption from 250 to 750 nm. UV-Vis spectra of solid samples were acquired on films of *ca.* 100 μm thickness placed over quartz slides.

Liquid phase photoluminescence spectra were acquired on a Horiba Fluorolog 3 spectrometer. The light source was a 450 W Xenon lamp, and the detector was a FL-1030-UP photomultiplier. The excitation wavelength was 310 nm, and the fluorescence intensity was measured from 360 to 600 nm.

In situ photoluminescence spectra were acquired on an Ocean Optics USB4000-FL spectrometer, with an Ocean Optics LS-310 LED light source at an excitation wavelength of 310 nm, and an Ocean Optics QR230-7-XRS SMA 905 optical fibre. The spectra were acquired by measuring films that were either placed on a black piece of paper or during uniaxial tensile tests carried out in a LINKAM TST350 microtensile stage with a 20 N loading cell. The stage was controlled by the LINK software. A pre-load of *ca.* 0.1 N was applied prior to tests to ensure that the sample was well loaded on the tensile stage. Rectangular samples of *ca.* 30 × 5 × 0.1 mm (length × width × thickness) were used and the strain rate was 50% min^{-1}. In order to allow the comparison of different emission spectra shown within a given figure, in particular the fractions of monomer and excimer emission, in each graph the spectra were normalized to the intensity of the monomer peak at 397 nm, which is the monomer band that is least affected by possible internal absorption effects.

Thermogravimetric analysis (TGA) curves were measured in air on a Mettler–Toledo STAR thermogravimetric analyser from

Open Access Article. Published on 06 February 2024. Downloaded on 9/15/2025 9:44:22 AM. This article is licensed under a Creative Commons Attribution-NonCommercial 3.0 Unported Licence.

room temperature to 600 °C, using a heating rate of 10 °C min^{-1}.

Differential scanning calorimetry (DSC) measurements were recorded in air on a Mettler–Toledo STAR system, with heating/cooling rates of 10 °C min^{-1}, from −80 to 200 °C. The glass transition temperature (T_g) was reported as the midpoint of the step change in heat capacity.

Fluorescence microscopy images were acquired at 20× magnification using an Olympus BX51 microscope equipped with an Olympus DP72 high-resolution camera. Images were recorded with a wideband UV filter (λ_{ex} = 330–385 nm; λ_{em} = 420–900 nm, Olympus U-MWU2).

Elemental analysis (EA) was performed by the Molecular and Biomolecular Analysis Service MoBiAS at ETH Zurich, Switzerland, and used to determine the C and H content of **Py-PEB**.

Methods

Solvent-casting of films of polymer/Py-PEB blends

Films of blends of the different host polymers and **Py-PEB** (0.5–10 wt% in the case of PI, 0.5 and 1 wt% in the case of PCL, and 0.1–1 wt% in the case of PU) were solvent-cast from THF solutions. The respective polymer (*ca.* 300 mg) and a solution of the appropriate amount of **Py-PEB** in 15 mL of THF were added to a 20 mL glass vial equipped with a magnetic stir bar and the mixture was stirred in the capped vial on a stirring plate for 1–3 days. If the polymer had not completely dissolved at this point, the vial was heated with a heat gun for a few seconds. The solutions were then cast into poly(tetrafluoroethylene) (PTFE) dishes (6 cm diameter) and the solvent was evaporated overnight in a fume hood. The resulting films were then transferred to a vacuum oven and dried overnight at 40 °C under reduced pressure.

Compression-moulding of polymer/Py-PEB films

The solvent-cast films were compression-moulded using a Carver 3851-0 hydraulic hot press (Indiana, USA). The films were cut up into small pieces, which were sandwiched between 2 PTFE sheets, using 150 μm spacers. The PI/Py-PEB and PCL/Py-PEB films were processed at 100 °C with a final pressure of 2 metric tons for 10 min. The PU films were not compression-moulded.

Synthesis of Py-terminated telechelic poly(ethylene-*co*-butylene) (Py-PEB)

The synthesis of Py-PEB was adapted from a published procedure.[40] An excess of OH-terminated poly(ethylene-*co*-butylene) (OH-PEB) was dried in a glass vial in a vacuum oven overnight at 60 °C. After removal from the oven and cooling to ambient temperature, 1.84 g (0.61 mmol) of OH-PEB were added to a 10 mL round-bottomed flask equipped with a magnetic stir bar. Dry DCM (5 mL) was added under N_2 flow, and the mixture was stirred under an inert atmosphere until OH-PEB had fully dissolved. 1-Pyrenebutyric acid (591 mg, 2.05 mmol), *N*,*N*′-dicyclohexylcarbodiimide (DCC, 488 mg, 2.37 mmol), and 4-dimethylaminopyridine (DMAP, 165 mg, 1.35 mmol) were added to a 250 mL round-bottomed flask under N_2 flow, and dissolved in 120 mL of dry DCM. The OH-PEB/DCM solution was added dropwise to the same flask. The reaction mixture was stirred for 24 h at room temperature under an inert atmosphere. At this point, ^{1}H NMR spectra showed that about 63% of the OH groups (the degree of functionalization was calculated *via* the resonance of the protons alpha to the OH groups) had reacted with 1-pyrenebutyric acid. Therefore, another aliquot of DCC (499 mg, 2.42 mmol), dissolved in 5 mL of dry DCM under N_2, was added. After stirring the reaction mixture for another 4 h, the reaction was stopped by cooling the reaction mixture to −20 °C. The mixture was kept at −20 °C for 60 h, to induce precipitation of dicyclohexyl urea, which was then filtered off. Subsequently, DCM was removed *in vacuo*, and the crude product was dispersed in a few mL of toluene. A small amount of Sudan Black (M_n = 456.54 g mol^{-1}) was added to colour the mixture and facilitate purification *via* size-exclusion column chromatography (Bio-Beads™ SX-1, 200–400 mesh; toluene). Toluene was evaporated *in vacuo*, and the product was dried in a vacuum oven overnight at 70 °C, which yielded Py-PEB (680 mg, 0.019 mmol, 32% yield) as a dark yellow, blue fluorescent, viscous liquid, which was characterized by ^{1}H NMR spectroscopy, ^{13}C-NMR spectroscopy, FTIR spectroscopy and elemental analysis. ^{1}H-NMR (400 MHz, $CDCl_3$): δ = 8.32–7.85 (m, 18H, ArH), 4.14–4.07 (m, 4H, CH_2–O), 3.40 (t, 4H, CH_2), 2.46 (t, 4H, CH_2), 2.20 (tt, 4H, CH_2), 2–0.5 (m, CH_2, CH_3, backbone). ^{13}C-NMR (101 MHz, $CDCl_3$): δ = 173.71 (C═O, ester), 135.92–123.49 (aromatic carbons), 39.05–26.05 (CH_2, polymer backbone), 11.04–10.70 (CH_3, polymer backbone). FTIR (cm^{-1}): 843, 1146–1262, 1382, 1461, 1738, 2853, 1922, 2960. Elemental analysis: anal. calcd for $(C_{20}H_{15}O_2)_2(C_4H_8)_{55}$: C = 84.97, H = 12.80. Found: C = 85.16 ± 0.01, H = 12.84 ± 0.11.

Author contributions

C. W., M. O., and J. M. C. contributed to the conceptualization of the present study and designed the experiments. M. O. carried out the experiments. M. O. processed the data under the supervision of C. W. and J. M. C. C. W., M. O., and J. M. C. wrote the manuscript. C. W. and J. M. C. supervised and funded the project.

Data availability

The source data of this study are available from the Zenodo repository at DOI: 10.5281/zenodo.10276391.

Conflicts of interest

There are no conflicts to declare.

 This journal is © The Royal Society of Chemistry 2024

Open Access Article. Published on 06 February 2024. Downloaded on 9/15/2025 9:44:22 AM.
This article is licensed under a Creative Commons Attribution-NonCommercial 3.0 Unported Licence.

Acknowledgements

The authors gratefully acknowledge financial support from the Swiss National Science Foundation (SNSF) through grants to J. M. C. (PRIMA PR00P2_208616), C. W. (200020_207796) and the National Centre of Competence in Research (NCCR) Bio-inspired Materials (51NF40-182881), and thank the Adolphe Merkle Foundation for funding. The authors are also grateful to Dr Derek Kiebala for sharing the Python script used to translate the photoluminescence spectra recorded into I_E/I_M values and correlating these to the stress/strain curves.

References

1 Y. Chen, C. J. Yeh, Q. Guo, Y. Qi, R. Long and C. Creton, *Chem. Sci.*, 2021, **12**, 1693.
2 Y. Huang, S. Huang and Q. Li, *ChemPlusChem*, 2023, **88**, e202300213.
3 Y. Chen, M. Sommer and C. Weder, *Macromol. Rapid Commun.*, 2021, **42**, 2000685.
4 G. De Bo, *Macromolecules*, 2020, **53**, 7615.
5 D. A. Davis, A. Hamilton, J. Yang, L. D. Cremar, D. Van Gough, S. L. Potisek, M. T. Ong, P. V. Braun, T. J. Martínez, S. R. White, J. S. Moore and N. R. Sottos, *Nature*, 2009, **459**, 68.
6 Y. Chen, A. J. H. Spiering, S. Karthikeyan, G. W. M. Peters, E. W. Meijer and R. P. Sijbesma, *Nat. Chem.*, 2012, **4**, 559.
7 K. Imato, A. Irie, T. Kosuge, T. Ohishi, M. Nishihara, A. Takahara and H. Otsuka, *Angew. Chem.*, 2015, **127**, 6266.
8 R. Göstl and R. P. Sijbesma, *Chem. Sci.*, 2016, **7**, 370.
9 J. R. Hemmer, C. Rader, B. D. Wilts, C. Weder and J. A. Berrocal, *J. Am. Chem. Soc.*, 2021, **143**, 18859.
10 M. Raisch, W. Maftuhin, M. Walter and M. Sommer, *Nat. Commun.*, 2021, **12**, 4243.
11 R. Kotani, S. Yokoyama, S. Nobusue, S. Yamaguchi, A. Osuka, H. Yabu and S. Saito, *Nat. Commun.*, 2022, **13**, 303.
12 Y. Sagara, M. Karman, E. Verde-Sesto, K. Matsuo, Y. Kim, N. Tamaoki and C. Weder, *J. Am. Chem. Soc.*, 2018, **140**, 1584.
13 Y. Sagara, H. Traeger, J. Li, Y. Okado, S. Schrettl, N. Tamaoki and C. Weder, *J. Am. Chem. Soc.*, 2021, **143**, 5519.
14 H. Traeger, D. J. Kiebala, C. Weder and S. Schrettl, *Macromol. Rapid Commun.*, 2021, **42**, 2000573.
15 H. Traeger, Y. Sagara, D. J. Kiebala, S. Schrettl and C. Weder, *Angew. Chem. Int. Ed.*, 2021, **60**, 16191.
16 J. Li, C. Nagamani and J. S. Moore, *Acc. Chem. Res.*, 2015, **48**, 2181.
17 C. Calvino, L. Neumann, C. Weder and S. Schrettl, *J. Polym. Sci., Part A: Polym. Chem.*, 2017, **55**, 640.
18 N. Deneke, M. L. Rencheck and C. S. Davis, *Soft Matter*, 2020, **16**, 6230.
19 Y. Chen, G. Mellot, D. Van Luijk, C. Creton and R. P. Sijbesma, *Chem. Soc. Rev.*, 2021, **50**, 4100.
20 F. Ciardelli, G. Ruggeri and A. Pucci, *Chem. Soc. Rev.*, 2013, **42**, 857.
21 C. Löwe and C. Weder, *Adv. Mater.*, 2002, **14**, 1625.
22 C. Löwe and C. Weder, *Color Tunable Photoluminescent Blends*. *US Pat.*, 7223988, 2007.
23 F. Cellini, L. Zhou, K. Sachin, S. D. Peterson and M. Porfiri, *Mech. Mater.*, 2016, **93**, 145.
24 T. Wang, N. Zhang, Y. Ge, C. Wang, Z. Hang and Z. Zhang, *Macromol. Chem. Phys.*, 2020, **221**, 1900463.
25 A. Pucci, *Sensors*, 2019, **19**, 4969.
26 Y. Sagara, S. Yamane, M. Mitani, C. Weder and T. Kato, *Adv. Mater.*, 2016, **28**, 1073.
27 J. Kunzelman, B. R. Crenshaw, M. Kinami and C. Weder, *Macromol. Rapid Commun.*, 2006, **27**, 1981.
28 M. Kinami, B. R. Crenshaw and C. Weder, *Chem. Mater.*, 2006, **18**, 946.
29 B. R. Crenshaw and C. Weder, *Macromolecules*, 2006, **39**, 9581.
30 F. Cellini, S. Khapli, S. D. Peterson and M. Porfiri, *Appl. Phys. Lett.*, 2014, **105**, 061907.
31 C. Calvino, Y. Sagara, V. Buclin, A. P. Haehnel, A. del Prado, C. Aeby, Y. C. Simon, S. Schrettl and C. Weder, *Macromol. Rapid Commun.*, 2019, **40**, 1800705.
32 D. J. Kiebala, Z. Fan, C. Calvino, L. Fehlmann, S. Schrettl and C. Weder, *Org. Mater.*, 2020, **02**, 313.
33 D. J. Kiebala, R. Style, D. Vanhecke, C. Calvino, C. Weder and S. Schrettl, *Adv. Funct. Mater.*, 2023, 2304938.
34 J. D. Eshelby, *Proc. R. Soc. London, Ser. A*, 1957, **241**, 376.
35 J. B. Birks, D. J. Dyson and I. H. Munro, *Proc. R. Soc. London, Ser. A*, 1963, **275**, 575.
36 N. A. A. Rossi, E. J. Duplock, J. Meegan, D. R. T. Roberts, J. J. Murphy, M. Patel and S. J. Holder, *J. Mater. Chem.*, 2009, **19**, 7674.
37 D. R. T. Roberts, M. Patel, J. J. Murphy and S. J. Holder, *Sens. Actuators, B*, 2012, **162**, 43.
38 C. Micheletti, V. A. Dini, M. Carlotti, F. Fuso, D. Genovese, N. Zaccheroni, C. Gualandi and A. Pucci, *ACS Appl. Polym. Mater.*, 2023, **5**, 1545.
39 D. Rasch and R. Göstl, *Org. Mater.*, 2022, **4**, 170.
40 S. Philip and S. Kuriakose, *J. Fluoresc.*, 2019, **29**, 387.
41 Z. Ji, Y. Li, Y. Ding, G. Chen and M. Jiang, *Polym. Chem.*, 2015, **6**, 6880.